Proton Effects in Charge-Coupled Devices

G. R. Hopkinson, *Member, IEEE,* C. J. Dale, and P. W. Marshall, *Member, IEEE*

Abstract— **Basic mechanisms and ground-test data for radiation effects in solid-state imagers are reviewed, with a special emphasis on proton-induced effects on silicon charge-coupled devices (CCD's). For the proton fluxes encountered in the space environment, both transient ionization and displacement damage effects arise from single-particle interactions. In the former case, individual proton tracks will be seen; in the latter, dark-current spikes (or hot pixels) and trapping states that cause degradation in charge-transfer efficiency will be observed. Proton-induced displacement damage effects on dark current and charge transfer are considered in detail, and the practical implications for shielding, device hardening, and ground testing are discussed.**

I. Introduction

BECAUSE of their sensitivity, ruggedness, and low power consumption, solid-state detector arrays are found in almost all present-generation satellite instruments used for high-resolution visible and infrared imaging (and also in many UV and X-ray instruments). Applications include spaceborne astronomy (as in the Hubble Space Telescope), Earth observation, surveillance, laser communications, and star trackers. The sensitive analog nature that makes them so useful, however, also makes them especially vulnerable to the effects of the natural space environment (and particularly to proton-induced displacement damage and transient effects). Hence, it is important that system engineers understand the trade-offs involved in choosing a device type or specifying a particular set of operating conditions, such as temperature and readout speed. The planning of a ground-test program and the proper extrapolation of the results to a prediction of on-orbit charge-coupled device (CCD) performance are also important parts of mission preparation. This review is, therefore, intended as a practical guide to radiation effects on solid-state imagers rather than a detailed discussion of basic mechanisms. This approach is helped by the fact that many excellent research papers have appeared in the published literature over the last few years so that, with a few notable exceptions (to be discussed later), the underlying physical interpretations are now reasonably well understood. It is hoped that this brief review will also give an introduction to this literature though, inevitably, the emphasis reflects the authors' own interests and experiences. For a more general discussion of radiation effects in imaging arrays, the reader is referred to [1] and [2] and the references therein.

Solid-state imaging detectors (sometimes called focal-plane arrays) contain a matrix of up to several million photosensitive elements (or pixels), each of linear dimension in the range 5–50 μm. The photogenerated charge is usually converted to a voltage and multiplexed to a small number of output amplifiers. There are a variety of different device architectures and detector materials available and these will be briefly discussed, from a radiation effects point of view, in Section III. The most commonly used array for imaging in the visible region is the silicon CCD.

In a space environment, we are mainly interested in effects due to the electrons and protons that exist in the Earth's trapped radiation belts or arise from solar flares. Trapped electrons are important for some orbits (e.g., geosynchronous) but are usually absorbed in the large amounts of shielding that surround the focal plane (often equivalent to more than 8-mm aluminum). In contrast, the trapped and flare protons have energies of up to several hundred MeV and are very penetrating and cannot be effectively shielded against. In this paper, we will concentrate, therefore, mainly on proton effects in CCD's, although the same basic phenomena (total dose effects, bulk displacement damage, and transient charge production) are also encountered to varying degrees with electron (or gamma) irradiation. Proton-induced single events will be emphasized and discussed in terms of their production of transient signal charge, and their permanent introduction of bulk damage, which generates dark current and traps signal charges.

Protons also deliver significant total ionizing dose (TID) to CCD's on-orbit, but this is not the major concern for many applications. It is possible to harden CCD's at both the device and system level against TID effects if they are important. Still, it is necessary to recognize the impact of ionizing dose on CCD's, and these effects are briefly discussed in the following section.

II. Basic Mechanisms

The basic mechanisms that occur when a particle track passes though a CCD are illustrated in Fig. 1 and discussed below.

A. Total Ionizing Dose Effects

Because most solid-state detector arrays use the metal-insulator-semiconductor structure for either photo-detection or readout (or both), these devices are susceptible to ionization damage within the insulator layer. With visible CCD's the gate dielectric is usually either silicon dioxide or a combination of silicon dioxide and silicon nitride. Infrared devices sometimes employ other materials. In understanding effects in these gate insulators, we can take as a model the vast body of experience on total ionizing dose effects on metal-oxide-silicon

Manuscript received August 14, 1995.

G. R. Hopkinson is with Sira Limited, Chislehurst, Kent, BR7 5EH, UK.
C. J. Dale is with the Naval Research Laboratory, Washington, DC 20375 USA.
P. W. Marshall was with the Naval Research Laboratory and is now with SFA Inc., Landover, MD 20785 USA.

Publisher Item Identifier S 0018-9499(96)03320-5.

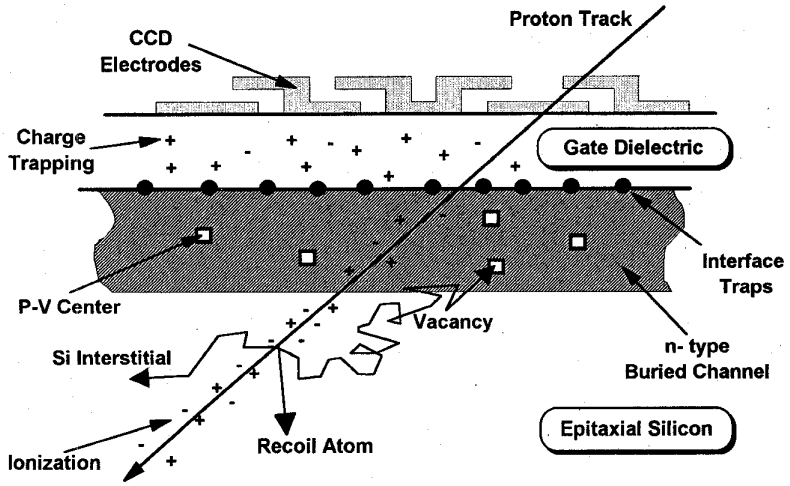

Fig. 1. Schematic diagram of the processes taking place when a proton passes through a CCD. These are charge trapping in the gate, and interface trap generation (ionization damage), ionization in the silicon (transient effects), and displacement damage in the silicon, which produces vacancy/interstitial pairs and stable defects such as the E center. Note that since the gate dielectric is usually composed of an oxide and a silicon nitride layer, both holes and electrons can be trapped.

(MOS) devices. Many excellent reviews are available (see, for example, [3]–[7]). The main effects are the buildup of trapped charge in the oxide and the generation of traps at the silicon dioxide/silicon interface. In an imager, these produce shifts in flatband voltages (i.e., the effective bias voltages applied to the device are changed) and increases in the surface dark current (i.e., the component of thermal dark current that is generated at the silicon dioxide/silicon interface). These effects are relatively well understood in CCD's and, in principle, can be reduced by appropriate choice of device architecture and oxide technology. Hence, performance in space is not ultimately limited by total ionizing dose effects.

Most gate dielectrics in commercial CCD's are thick (~100 nm) and radiation-soft, so that for a device biased during irradiation, a typical shift in flatband voltage is 0.1 V/krad(Si) (and roughly half that for an unbiased device). For total doses above about 10 krad, we start to see changes in performance (particularly in the operating point of the output amplifier). The device, however, will probably be functional up to several 10's of krad(Si) [maybe 100 krad(Si) if bias voltages are adjusted in flight]. Devices are starting to become available with more radiation hard oxides so that performance is possible up to 1 Mrad(Si) [8]. Post-irradiation (i.e., annealing) effects are not usually significant for flatband shifts in commercial CCD oxides [9], [10].

Depending on the device type used, the ionization-induced surface dark current density can be extremely important [typical increases are in the range 1–10 nA/cm^2/krad(Si) at 20°C]. If, however, the CCD is biased so that the silicon surface is inverted, then holes from the channel stop regions fill the interface traps and suppress the generation of dark current [11]. This can be achieved with multiphase pinned (MPP) devices [12] or with a technique known as dither clocking or dynamic dark-charge suppression [10], [13], [14]. With modern devices and optimized clocking, the loss in full well capacity that accompanies MPP operation need not be more than 20%. Use of dither clocking to swap between integration phases can result in dark-current nonuniformity, but appropriate choice of clock levels can ameliorate this problem. Further discussion of these techniques is beyond the scope of this paper. For our purposes, it is sufficient to say that, for low total-dose applications, operation in inversion can almost totally remove the ionization-induced dark current, leaving only the component that arises in the bulk of the depletion layer as a result of particle-induced displacement damage. At high total doses, it should be remembered that the flatband shift can sometimes be enough to take the device out of inversion.

B. Transient Effects

Transient radiation effects are due to the ionization-induced generation of charge within the active region of a detector (for example, the epitaxial silicon layer of a CCD). The effects are not permanent, and the spurious charge is swept out during readout, but the additional charge constitutes a significant source of noise in the video data. For particle (e.g., proton) irradiation, electron-hole pairs are produced along the entire length of the particle track. To a first approximation, the energy deposited in the silicon depends on the product of the ionizing energy loss, dE/dx, of the particle and the track length. The average energy loss can be found using codes such as TRIM (transport of ions in matter [15]). Fig. 2 shows the average ionizing energy loss for protons in silicon in units of MeV cm^2/g (often termed the linear energy transfer, or LET). The energy required to generate each electron-hole pair is often assumed to be roughly three times the bandgap, though this is a very approximate rule and has been experimentally verified for only a few materials. Where experimental data is available, this should be used in preference: for silicon, we have approximately one electron-hole pair created for every 3.62 eV ionizing energy deposited at 20°C.

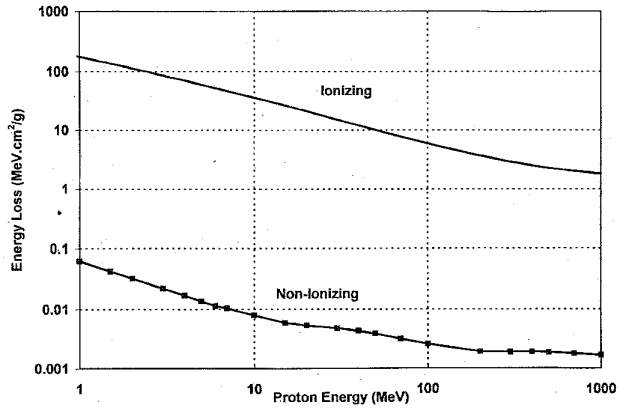

Fig. 2. Nonionizing energy loss (NIEL) (from [32]), and ionizing energy loss (i.e., LET), calculated using TRIM [15].

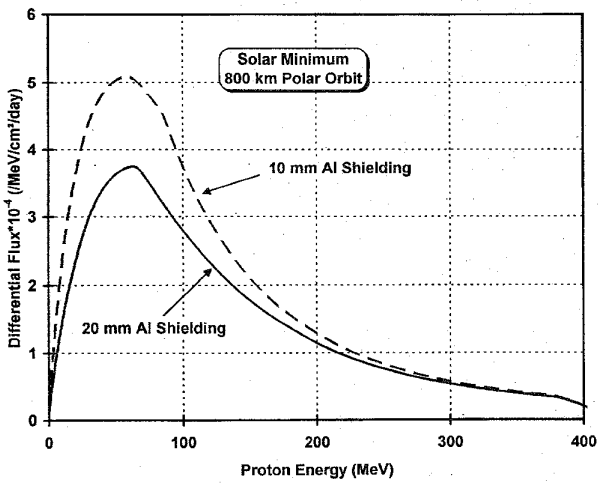

Fig. 3. Differential proton spectra for an 800-km polar orbit, assuming 10- and 20-mm aluminum shielding.

It can be seen from Fig. 2 that, for the range of energies of interest, the higher the energy of the incident proton, the less will be the energy deposited per micrometer of track. Even for energies of several hundred MeV, however, the number of electron-hole pairs created is greater than 100 μm, so that for a typical CCD charge-collection depth of 20 μm, a proton transient will generate at least 2000 electrons. Because full well capacities are typically no more than 5 $\times 10^5$ electrons, each proton strike results in a significant signal.

The problem is compounded because of variations in the amount of charge deposited in each pixel. These arise primarily because, in a space environment, there is a large spread in the energy of the incident protons (as seen in the example of Fig. 3, discussed below). Even in the case of ground-based testing with monoenergetic protons, however, one would expect to observe fluctuations in the amount of charge deposited in a pixel by incident particles. A general theoretical treatment based on the work of Kellerer [16], together with experimental verification, has been given by Burke *et al.* [17]. This work treats the case of gamma-ray interactions with CCD's, but as the authors point out, the basic principles also apply to charged particle-induced transients. The three basic factors contributing to variations in transient signal size for monoenergetic protons are the following.

1) A detector in an omnidirectional environment will experience a variety of track lengths. Track length distributions have been given for rectangular parallelepiped geometries by Vickers *et al.* [18] and Bradford [19] (with typographical corrections as given by Ziegler and Landford [20]). Langworthy [21] has discussed the extension to the more realistic case of active volumes with rounded corners. Whatever theory is used, the root mean-square variation in track length is comparable with the average value (which, for a convex volume, is given by 4 $\times$ the volume divided by the surface area). So within a particular pixel of dimensions 20 μm $\times$ 20 μm $\times$20 μm we can expect fluctuations in track length of order 10 μm.
2) For those parts of the track that are deeper than the depletion layer, there will be lateral spreading (to adjacent pixels) because of charge diffusion [22]–[24]. The charge generated in the heavily doped substrate beneath the epi layer (typically $\sim$15 μm thick) quickly recombines and is not collected. The effective minority carrier diffusion length, however, can be many times the thickness of the field-free region beneath the depleted pixel volume. This significantly affects the amount of charge collected and results in charge collection by more than one pixel.
3) There is a spread in the energy lost by an ion (an effect known as energy-loss straggling). In addition, some of the energy is carried outside the sensitive volume by long-range secondary electrons. For example, Xapsos [25] estimates that, for the case of 100 MeV protons incident on a sensitive volume with an average path length of $\sim$10 μm, the fluctuations in energy loss will be comparable with the mean energy loss and that 10% of the energy will be carried away by long range electrons. These estimates, however, would be difficult to corroborate in laboratory measurements on CCD's because the sensitive volumes are not precisely known and diffusion effects are difficult to model with great accuracy.

In a space environment, the effects of variations in the proton energy and path length are by far the most important. Heavy-ion transient events from cosmic rays will also occur, though in greatly reduced numbers, as compared to proton events. Lomheim *et al.* [26] have carried out an experimental investigation of single-particle transient signals from monoenergetic protons and heavy ions incident at various incident angles to a Kodak KAF-1400 CCD. The results were in agreement (to within 20%) with the signal charge expected for a particular ion track length including contributions from the pixel depletion and diffusion volumes. McCarthy *et al.* [27] have performed a similar investigation (using protons in the range 50–300 MeV) for a deep depletion CCD, specially designed for X-ray astronomy. They found that in many cases the proton events could be distinguished from their X-ray

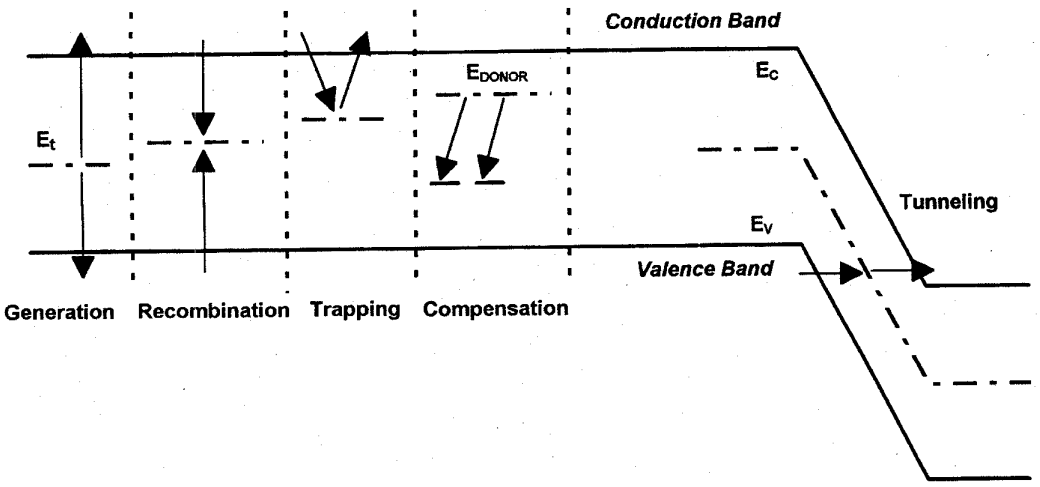

Fig. 4. Illustration of the five basic effects of a defect energy level (E_t) on the electrical performance of a device (after [5]).

signals. However, in general, the large spread in the amount of charge deposited in a CCD makes it very difficult to discriminate against proton transients. Any attempt to partially filter proton transients by increasing the detection threshold will result in a reduced sensitivity that is often unacceptable. Another way of mitigating the effects is to use a thinner active volume so that the track lengths are shorter, but this will reduce the detector responsivity for wave lengths absorbed deep in the device (i.e., in the red for a front-illuminated CCD).

In order to estimate the number of tracks due to interactions with trapped or solar flare protons, we can start with the orbit averaged differential proton flux (in protons/MeV/cm^2/day) after passage through the instrument shielding. The area under the curve is the total flux of particles that pass though the shielding. This flux, however, is not uniform over time [28]. For instance, in low Earth orbits, the main contribution comes during passage though the South Atlantic anomaly (SAA). As an example, we take the case of a polar orbit at 800-km altitude. Fig. 3 shows the differential fluxes during solar minimum after passage through spherical shields of 10- and 20-mm aluminum, as calculated using the space radiation code [29] (in turn based on the earlier AE-8, AP-8, and CREME models). For the 10-mm shield, the total flux of 0.78 $\times 10^7$ protons/cm^2/day at solar minimum is obtained during SAA passage, which takes $\sim$0.1 h out of a 1.68-h orbit. Hence, the average flux during transit through the SAA is 1500 protons/cm^2/s. For an integration time of 1 s and a pixel size of 20 μm $\times$20 μm, we have an event rate of one in 170 pixels. This would be enough to seriously impair the quality of CCD images. Instruments (e.g., star trackers) that continuously stare at a scene, however, will often have software that discriminates against signals that are only present for a single image frame, thus enabling objects to be tracked during passage through the SAA. If the observing situation allows, this is the best way of ensuring a tolerance to transient effects. Nevertheless, it is difficult to operate CCD's in the heart of the trapped radiation belts where fluxes can be one-to-two order-of-magnitude higher than in the SAA.

C. Displacement Damage

Displacement damage in semiconductors has been reviewed by Summers [30] and Braunig and Wulf [7]. When protons (or any other particles) pass through semiconductor material, nearly all the energy loss goes into ionization and the creation of electron-hole pairs, as discussed above. There is, however, a small fraction that goes into the displacement of atoms from their lattice sites and the creation of vacancy-interstitial pairs. This fraction is called the nonionizing energy loss, or NIEL, and has been calculated for silicon by Burke [31], with revised values given by Dale *et al.* [32]. Fig. 2 shows that, for silicon, roughly 0.1% of the total energy loss goes into the production of vacancies and interstitials. More than 90% of these recombine, but the remainder migrate through the lattice until they form stable (i.e., relatively long-lived and immobile) complexes. The defects produced will have energy levels within the bandgap and can give rise to any of the following five effects illustrated in Fig. 4 [5]:

generation of e–h pairs
recombination of e–h pairs
trapping of carriers
compensation of donors or acceptors

and

tunneling of carriers

depending on the temperature, carrier concentration, and the location at which the defect resides. In a CCD, the main effects are the generation of thermal dark charge within the depletion region and the trapping of signal charge within the n-buried channel.

Only defects with energy levels close to midgap (which is 0.55 eV away from both the valence and conduction bands) are efficient at generating dark current, and it also turns out that it is usually midgap states that lead to traps with sufficiently long time constants to interfere with the charge-transfer process (see Section IV). In silicon, the relevant

defects are located at around 0.4 eV below the conduction band. They include the E center (also called the P–V center) [33], the substitutional phosphorus-interstitial carbon (P_s, C_i) pair [34], the divacancy [35] and, as has recently been suggested [36], a higher-order vacancy complex. Because the energy levels of these defects are similar, so are the effects on dark current generation and charge trapping. They do differ, however, in their annealing characteristics (i.e., their long-term stability at increased temperatures), and in their introduction rates (i.e., the number produced per cm^3, divided by the particle fluence). These differences in defect behavior are important when characterizing the damage in individual pixels (e.g., for dark current spikes), or when developing hardening approaches that utilize on-orbit annealing of the CCD. The total inventory of defects has not yet been characterized in detail, but experimental evidence, to be discussed below, indicates that CCD performance is primarily influenced by the P–V center. This is not surprising since phosphorus is the dopant used to form the n-buried channel.

The important point about proton NIEL is that (for silicon at least) it appears to be proportional to the total number of stable defects created. This number does not depend (to a first approximation) on the details of the interaction process [37], [38]. A recent study [39] has extended this correlation to cover a wide range of energies and particle types. These results imply that, on average, the electrical properties of the stable defects are similar, whether the original vacancy-interstitial pairs are created in dense clusters (as happens when there is an inelastic reaction between the incoming proton and an Si nucleus) or whether the displacements are more spread out (as happens with elastic coulomb reactions that occur more frequently but do not deposit much energy). This is borne out by experimental measurements of global CCD parameters, such as average dark current [40] and charge transfer efficiency [41], [42]. These have been found to be proportional to the NIEL, which represents the average displacement-damage energy loss rate. On the other hand, we shall see in a later section that descriptions of the pixel-to-pixel variations in properties, such as the dark current, require a knowledge of the recoil damage spectra associated with the NIEL calculation, or else a Monte Carlo calculation of the proton-induced damage events.

Because of the correlation between CTE or dark-current damage and NIEL, we do not need to be concerned with the actual number of defects created. This is fortunate since this number depends on many factors. Instead, we can use the NIEL to extrapolate from direct measurements. This can be done in several ways. Ideally, when studying a new device type (and certainly when looking at new materials), radiation tests should be performed at several proton energies so as to map out the energy dependence of the damage factor (the bulk dark-current generation or the CTE degradation per incident proton). If there is confidence that there is proportionality between damage and NIEL, then testing can be performed at just one proton energy (so as to establish the scaling factor). If the damage factor, K_p, is known from ground testing at this proton energy, E_{test} (e.g., 10 MeV), then effects can be estimated for a given mission by first calculating the differential proton flux $[d\Phi(E)/de]$ behind the spacecraft shielding (as in the examples of Fig. 3), multiplying this spectrum by the NIEL at each energy, and then dividing by the NIEL at the test energy, 0.007 885 MeV cm^2/g at 10 MeV [28] (Fig. 5). The area under the resulting curve is the equivalent number of protons at the test energy, and the mission damage is found by multiplying by the damage constant (K_p) and the mission duration (t_m). Expressing this analytically we have

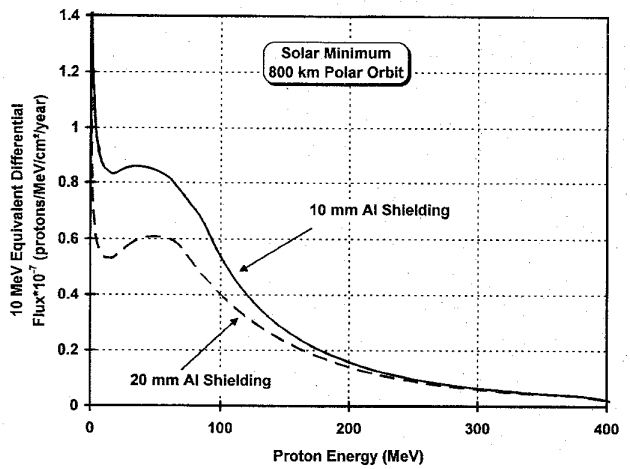

Fig. 5. The product of the NIEL (from Fig. 2) and the differential proton spectra of Fig. 3 divided by the NIEL of 10-MeV protons. This gives the NIEL equivalent differential flux of 10-MeV protons.

$$\text{mission damage} = t_m \int_0^\infty K_p \frac{NIEL(E)}{NIEL(E_{test})} \cdot \frac{d\Phi(E)}{dE} \cdot dE. \quad (1)$$

With this model we can estimate the amount of damage for various proton spectra and shield thicknesses, so it is useful for both space predictions and planning of ground tests.

The approach requires a high-enough test energy that protons are not significantly slowed down in the active region of the CCD so there is a constant energy-loss rate within the sensitive volume. This is discussed further in [38], [42]. Ten MeV is often a convenient energy to choose. It has the advantage that the range of the silicon recoils will usually be less than the dimensions of the sensitive volume. Though this is not important for average dark charge (or CTE), it is relevant when looking at pixel-to-pixel variations (as discussed in detail in [32]).

Note that the concept of nonionizing energy deposition plays the same role in displacement damage effects as ionizing energy deposition (i.e., LET) plays in ionizing effects (such as flatband voltage shift). In terms of definitions and units, the displacement damage does not have to be referred to a specific test energy [as has been done in (1)]. It can be treated in a manner analogous to ionizing dose (as discussed in [38], [42], [43]).

In the above, it has been neglected that secondary neutrons will be created as the incident protons pass through the shielding material. These will also produce displacement damage; in fact, the secondary neutron damage will tend to dominate the primary proton damage if thick shields of dense materials

such as tantalum are used. Dale *et al.* [38], [42] have shown that for a 705-km polar orbit, the secondary neutron damage is significant for Ta thicknesses of 1 cm or more (so that use of thicker shields brings little or no benefit); whereas, if aluminum is used as the shielding material, then neutron production is not important (at least for any shield thickness of practical interest). The advantage of using dense-shielding materials is that, even though their effectiveness *per unit mass* is lower than for aluminum (both for displacement and ionization effects), their efficiency *per unit volume* is higher. Hence, dense shields can often be placed in restricted volumes close to the detector, thereby keeping the surface area (and the total mass) down. There is clearly a limit, however, to the thickness that is practically useful.

III. Device Architectures and Radiation Effects

Before discussing in detail the effects of displacement damage on the performance of silicon CCD's, we will provide an overview of the radiation response of two major categories of solid-state imagers, those that operate in the visible/UV part of the spectrum and those which are sensitive in the infrared.

A. Devices for Detection in the Visible/UV Regime

The device most commonly used in visible and UV detection is the buried-channel CCD (Fig. 1). It has a shallow ($\sim 1\,\mu$m) n-type layer implanted just beneath the surface of the silicon. Since the potential minimum is just below the surface, the stored charge is kept away from trapping states (either process- or radiation-induced) at the Si/SiO_2 interface. Surface-channel CCD's have signal charge stored at the surface where it can come into contact with surface traps and have correspondingly lower charge-transfer efficiencies (CTE's). They have the advantage, however, of a charge-storage capacity roughly an order of magnitude higher than the buried-channel CCD [44]. Hence, surface-channel CCD's are sometimes used as the readout multiplexer in infrared photodiode arrays, which are discussed in the next section.

Buried channel silicon CCD's are especially vulnerable to proton-induced displacement damage because of their high performance, which can easily be degraded. Modern devices can contain up to several million pixels, and devices have been reported with pixel arrays as large as 5120 × 5120 [45]). For these devices to operate properly, the density of trapping states in the buried channel must be *very* low. For example, to achieve <10% signal loss for 1000 transfers, we require a CTE of at least 0.9999 (i.e., $0.9^{0.001}$) per pixel transfer. This is easily achieved prior to irradiation because CTE values of greater than 0.999 995 are routinely obtained. For a signal size of 1000 electrons (typically contained in a volume of 50 μm^3), however, we require less than one radiation-induced trap every 10 pixels (or a density of $\sim 2 \times 10^9$ cm^{-3}), in order to maintain a CTE of 0.9999; assuming every trap within the volume captures an electron. Unfortunately, the proton exposure during a typical space mission can easily produce at least this density of defects in the buried channel. For example, Holland [46] has estimated that a 10-MeV proton fluence of 3.6×10^9 cm^{-2} [which corresponds to a total ionizing dose of 2 krad(Si)], creates 3×10^{10} E-centers/cm^3. Hence, there is potentially a serious problem with any instrument that requires good CTE performance in a space environment. There are, howver, several ways in which the effects of displacement damage can be reduced; these are discussed in Section IV. As an alternative, the charge-injection device (CID) does not rely on the charge-transfer process since signals are sensed directly on address lines connected to each pixel. The disadvantage of CID's is that they exhibit increased fixed pattern noise and increased noise due to the address line capacitance (though a nondestructive readout mode is commonly used so that signals can be repetitively read and averaged). Nevertheless, the lack of CTE effects makes these devices attractive for some applications [8].

Dark current is another CCD parameter that is greatly influenced by radiation. It arises either from interface traps at depleted surfaces, from generation centers in the depletion layer, or from diffusion from the bulk. At room temperature or below, only the first two mechanisms are usually important. As discussed in Section II, surface dark current can be suppressed by operating the surface in inversion (and dark-current suppression can also be achieved in some designs of linear-diode arrays where the surface is not depleted). For an inverted mode device, the average dark-current density is typically around 10 pA/cm^2 at 20°C, but even a single midgap state within a 20 μm × 20 μm pixel will give ~ 3 pA/cm^2 (assuming a capture cross section of 10^{-15} cm^2) [47]. Hence, we have a similar situation to CTE damage in which the occurrence of even a single defect within a pixel can be noticed, even though it may not be detrimental, depending on the particular application.

A third parameter that is affected by displacement damage is the noise of the output amplifier. In modern CCD's, it is common to use lightly doped drain (LDD) n-buried channel-depletion mode MOSFET amplifiers so as to achieve low noise performance. Excess low-frequency noise can be produced by displacement damage, and this can be important for low-noise instruments such as those used in spaceborne astronomy. However, the effects are generally only significant at a higher proton fluence than for CTE and dark-current variations. Murowinski *et al.* [48], [49], and Robbins [50] have discussed these effects, and they will not be considered further here. Following the next section, we concentrate on displacement damage effects on CTE and dark current in CCD's.

B. Devices for Infrared Imaging

Some of the most commonly employed imagers for the near-to-long wave length infrared are fabricated with various HgCdTe alloys, although InSb, InGaAs, and other materials are also used. Devices are usually formed as a hybrid of a detector array of either MIS capacitors or photodiodes and a silicon readout circuit optimized to handle large signal sizes, although monolithic IR CCD's and CID's can be manufactured (see, for example, [51]). It is, therefore, necessary to consider radiation effects both in the readout circuit and the detector elements. The radiation response of infrared devices is application and device dependent. For example, photovoltaic and photoconductive devices have different mechanisms for radiation-

induced performance degradation. Also, some effects, such as the low temperature TID response of MOS circuits and the surface tunneling via radiation-induced interface traps, are issues peculiar to IR devices.

It is to be expected that proton-induced displacement effects will not normally be important for silicon-readout circuitry for several reasons. Dark-current effects should be negligible because of low-operating temperatures, large signal levels, and high readout rates. Charge-transfer efficiency is either not applicable (in directly addressed CMOS or FET multiplexers) or will be intrinsically low because surface channel CCD's have been used to maximize signal capacity (in this case CTE will be affected by total ionizing dose but will only be significantly degraded further at high-dose levels). All of the readout devices, however, will still be susceptible to proton-induced transients (as in Section II-A), and total ionizing dose effects can be important in some cases ([52] gives an example). To date, little experimental work has been reported on permanent effects in IR multiplexers. Cluzel *et al.* [53] give results on total dose, dose rate, and neutron irradiation of a surface channel CCD (from Thomson-CSF, France). Though threshold-voltage shifts were observed, the overall effects on device performance were stated to be small.

As with multiplexers, there is little experimental data available in the open literature concerning radiation effects in infrared detector elements and almost no work on proton effects, in particular. This situation is expected to change as infrared arrays are utilized in applications such as Earth observation. In the meantime, some of the available radiation-effects literature is reviewed in [1], [2], [54]. Total ionizing dose will cause flatband voltage shifts and buildup of interface traps in passivating layers in a similar way to MOS devices. Transient events will lead to large signals since the bandgap is small (0.1 eV for a long-wave infrared HgCdTe detector with a cutoff wave length of 12 μm). In addition, displacement damage may be significant, especially for low-signal applications (although dark currents are normally intrinsically high because of process-induced defects).

IV. Displacement Damage Effects on CTE in CCD's

A. Definitions

Charge transfer efficiency (CTE) is one of the basic performance parameters of a CCD. It is defined as the fractional signal transferred from one pixel to the next. A related quantity is the charge transfer inefficiency or CTI (= 1 − CTE). For an unirradiated CCD, these parameters are usually regarded as constant, independent of signal size or operating conditions (provided that the manufacturers' stated maximum operating speed is not exceeded). For a proton environment (or when there are significant numbers of process-induced traps), the situation is very different. Displacement damage produces trapping defects, such as E centers, within the buried channel. The CTE is then governed by the dynamics of emission from and capture by these traps, rather than effects due to drift and diffusion as in classical CTE. In the case of trap-degraded CTE, it is necessary to imagine that the signal charge is moving through a sea of traps that are continuously emitting and capturing electrons. The amount of charge trapped and the particular pixel into which it is released, depends on the values of the emission and capture times, relative to the clocking rate of the CCD and the particular operation being performed. For example, the radiation performance would differ depending on whether we are considering serial or parallel charge transfers, slow line moves (for readout), or fast line moves (for charge dumping, frame transfer, or line binning). The CTE also becomes dependent on the signal size and the background charge (either provided by dark current or by a constant mean level in the particular scene being imaged).

CTE damage in CCD's has recently been studied by several authors, mostly for conditions in which the background charge is low ([38], [41], [42], [46], [55]–[58]), but also for cases where the background is significant [59]. These studies rely on the basic Shockley Read Hall (SRH) theory, as originally applied to buried channel CCD's by Mohsen and Thompsett [60].

For a trap located at an energy, E_t, below the conduction band and with a capture cross section, σ_n, the capture and emission times, τ_c and τ_e, are given by

$$\tau_c = \frac{1}{\sigma_n v_{th} n_s} \tag{2}$$

$$\tau_e = \frac{\exp\left(\frac{E_t}{kT}\right)}{\sigma_n X_n v_{th} N_c \chi} \tag{3}$$

where n_s is the signal density within the buried channel, v_{th} is the average thermal velocity for electrons, N_c is the effective density of states in the conduction band, T is the absolute temperature, and k is Boltzmann's constant. X_n is the entropy factor associated with the entropy change for electron emission from the trap, and χ is a field-enhancement factor to allow for any enhanced emission due to the Poole–Frenkel effect or to phonon-assisted tunneling, both of which occur in regions with an electric field greater than about 10^4 V/cm [61].

Measurements of emission time [57], [59] and annealing studies [63] have identified the dominant radiation-induced trap to be the phosphorus-vacancy center, which is located at $E_t = 0.44$ eV and has a cross section 3×10^{-15} cm^2.

It can be seen that the capture time depends inversely on the signal density and will be shortest in the center of a charge packet where the density is highest. Typically, we expect capture times of less than 100 ns for signals of 10 000 electrons [57], increasing to ~400 ns for a signal of 500 electrons. At the edge of a packet, however, where the density is low, the capture time can be several 10's of ms. Clearly, if charge is transferred through a pixel faster than it can be captured, then CTE will not be degraded, and we have a CTI capture factor, given by

$$\text{CTI capture factor} = \left[1 - \exp\left(\frac{-t_t}{\tau_c}\right)\right] \tag{4}$$

where t_t is a characteristic transfer time. In practice, this CTI factor will be close to one, unless we have fast clocking, such as in the case of a serial-readout register clocking at rates faster than one pixel/μs.

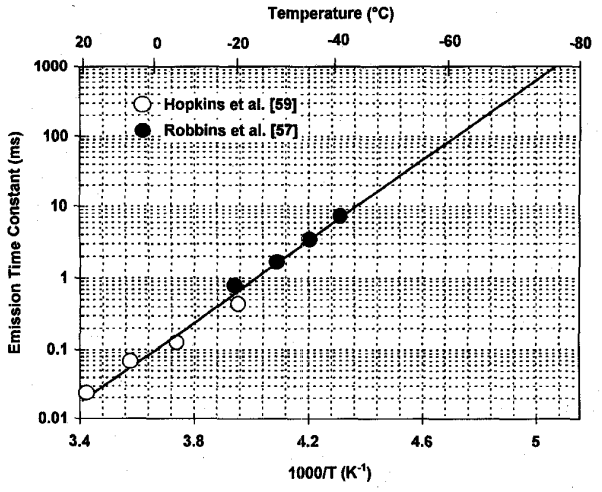

Fig. 6. Plot of trap emission times versus 1000/T from data of Hopkins *et al.* [59], and Robbins *et al.*[57].

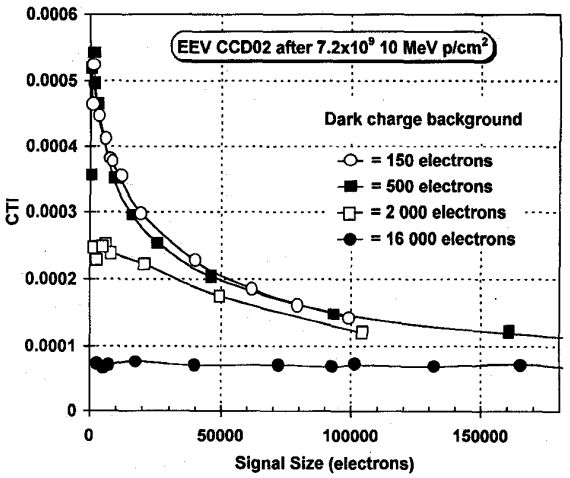

Fig. 7. CTI for an EEV CCD02 device induced by 7.2 $\times 10^9$ 10 MeV protons/cm^2 (equivalent to 4 krad) for various signal sizes and backgrounds. The dwell time per phase was 0.66 μs.

Equation (2) indicates that the capture time is only weakly dependent on the temperature through v_{th}, which is proportional to $T^{1/2}$ and σ_n, which can also be temperature dependent); whereas, τ_e (3) is exponentially dependent on temperature. Fig. 6 shows experimental measurements of the emission time constant for displacement-damaged CCD's [57], [59]. It can be seen that τ_e has a value of $\sim$400 μs at -20°C, decreasing to 20 μs at 20°C. Extrapolating the results to lower temperatures gives $\sim$1 s at -80°C. If the charge packets of interest (for example, X-ray events, star images or the highlights of an imaged scene) are moved through a pixel on average timescales, t_s, shorter than these emission times, then traps will be filled by the first (sacrificial) packet readout but will still be filled (they have not had sufficient time to emit) when subsequent packets arrive. The CTI emission factor is then given by

$$\text{CTI emission factor} = \left[1 - \exp\left(\frac{-t_s}{\tau_e}\right)\right]. \qquad (5)$$

This demonstrates the big advantage of cooling the CCD so that traps are effectively frozen out and remain permanently filled. Note that the emission time governs the number of pixels downstream of the charge packet that are affected by deferred charge. For example, we may have a 1000 $\times$ 1000 pixel CCD operated at -20°C at a readout rate of 1 pixel/μs. The emission time is then roughly 400 μs, and the time to read out one line is 1 ms. Hence, most of the charge trapped during a line move will be emitted (i.e., deferred) into only one subsequent line.

In contrast, if lines are transferred every microsecond, for example, during a frame transfer or for serial readout along the readout register, then charge will be deferred over $\sim$400 pixels. However, highlights (or events) must be separated by more than 400 pixels during such fast clocking, or the emission factor (5) comes into play. Note that for line moves during readout, which occur only every millisecond, there is no such restriction. Additional examples of the effect of clock rate on CTE have been given by Janesick *et al.* [12].

The effect of background charge has been considered in [59]. Fig. 7 shows that CTI can be dramatically decreased. This is because the background charge is present within a pixel for long periods of time and can be trapped into regions at the edges of a charge packet even though the capture time for these regions is long because of the low signal density [see (2)]. Thus, background charge is very effective in filling traps. In fact, for the CCD studied in [59] (a CCDO2 device from EEV, UK) the background charge was found to be five times as effective as signal charge for reducing CTI, for a typical operating condition.

B. Predicting Effects

Fig. 7 also indicates the magnitude of the radiation-induced CTI. The following example illustrates some of the issues involved in considering how these data might apply to making space predictions. The data in Fig. 7 were taken for conditions where the dwell time per clock phase was 0.66 μs, but Fig. 8 shows the effect of increasing this dwell time. For the same reason that background charge is effective in filling traps, if the signal charge is resident under a clock phase for an extended time, then charge will be trapped into an extended volume. More charge will be trapped and the CTI will increase by a factor of $\sim$2 in going to line move times of order 1 ms. For these conditions, we should take a CTI of $\sim$0.001 per pixel as a worst case (low background and low signal) and $\sim$0.0002 for a best case (for high signals or high background). This is after an equivalent 10-MeV fluence of 7.2 $\times 10^9$ cm^{-2} [which would give 4 krad(Si) of total ionizing dose to the oxide]. Hence, we have a worst-case damage constant (the change in CTI divided by the proton fluence) at 10 MeV of $\sim 1.5 \times 10^{-13}$ cm^2/proton, in good agreement with other measurements for low-background conditions [42]. This damage constant can then be substituted for K_p in (1) to derive the damage for a particular mission. For the high background case, the value of K_p is at least a factor five lower. Note that it is probably not possible to predict effects to better than a factor two to

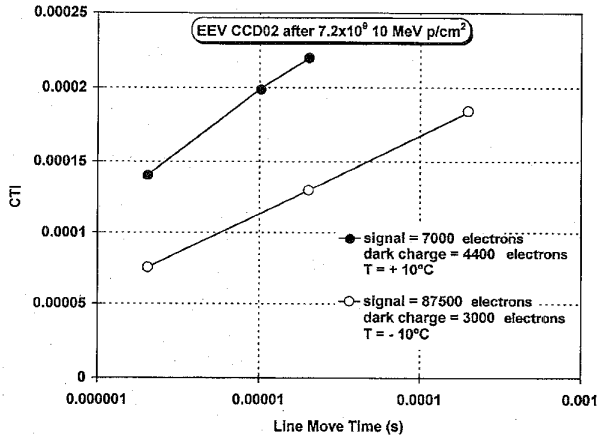

Fig. 8. As Fig. 7, but plotting CTI versus dwell time under an electrode for constant signal size and background (in electrons).

three from published data (even for a known environment), because of variations in the operating conditions (background and clocking rate) and in the measurement techniques used in a given laboratory. Variations due to device geometry and differing defect introduction rates may also be important in some cases. For these reasons, it is recommended, for critical space applications, that ground testing be tailored to reflect as closely as possible the on-orbit conditions.

C. Methods of Reducing CTE Degradation

There are several ways in which the effects of CTE damage can be reduced. If the signals to be measured are small (as in X-ray astronomy applications), then devices with a supplementary buried channel, or notch, can be used [41], [55], [62]. This is an additional phosphorus implant that confines small signals to a narrow region in the center of the buried channel. Because the signal charge is restricted to a smaller volume, fewer traps are encountered during transfer. In this way, up to an order-of-magnitude improvement in CTE performance can be achieved. The use of background charge (or fat zero) to fill the trapping states and improve CTE was discussed above. Note that this approach will usually carry the penalty of increasing the noise (because of the additional shot noise, on the background signal). If, however, the CCD is operated at a low enough temperature that the trap emission time is longer than the frame time, then injection of charge (for example via an injection gate) and flushing of charge through the CCD can fill the traps without an increase in noise [57]. Another method (suggested by Holland *et al.* [63]) is to periodically heat the device to about 100°C so as to anneal the E centers and reduce the damage.

D. Methods of Measuring CTE

Some of the more commonly used CTE measurement techniques are briefly described below. In making low-temperature ground-test measurements of radiation-induced CTE, a popular method is to plot the intensity and location of signals produced in the CCD via illumination by X-rays from a radioactive source [12], [41], [55]–[58]. These X-rays introduce well-defined amounts of charge (assuming that diffusion effects are allowed for). If slow-scan low-readout noise electronics is used, then very small changes in CTE can be detected. The method has also been extended to room temperatures [10]. Another method is the periodic pulse technique [60], whereby charge pulses are injected into individual pixels of the CCD (if the CCD has been designed to have the appropriate injection gate structure). There are several optical techniques for measuring CTE. For example, imaging of a bar pattern and measuring the contrast, or the extended pixel edge response or EPER [64] method (though it should be noted that this method will not be sensitive if the emission time is long and charge is spread over a large number of pixels). Finally, an optical technique has been described by Hopkins *et al.* [59], which involves spot illumination of the CCD, followed by repeated backward and forward charge transfer regimes (to increase the charge loss and improve the measurement accuracy). Note however that there are some types of advanced CCD architectures (designed to achieve both inverted mode operation and high full well capacity) where backward clocking (away from the readout register) is not possible and this method cannot be used.

V. Displacement Damage Effects on Dark Current in CCDs

A. Effect on Mean Value and Nonuniformity

As an example of the effect of displacement damage on mean dark-current level, Fig. 9 shows the increase in mean dark current density at 20°C for the image region of an MPP CCD as a function of proton fluence at 10 MeV. In this device, the surface dark current is suppressed because the surface is inverted [11], so that the dark current comes mainly from the bulk of the depletion layer (though there can be a small surface component due to incomplete inversion of the whole pixel area). The particular CCD is a 512 × 512 pixel TH7895M manufactured by Thomson-CSF Semiconducteurs Specifiques (France) but is typical of modern devices (the pixel size is 19 μm × 19 μm). The dark-current increase is characterized by the damage constant, K_p, which has a value of 2.8 $\times 10^{-11}$ nA/cm^2/proton/cm^2 in this example. The average on-orbit dark current behavior can be predicted using this damage constant in (1) of Section II-C. A similar value (within a factor 2) has been found by Dale *et al.* [40] for a CID.

The increase in mean dark current with proton irradiation is important, but of greater consequence is the large increase in dark current nonuniformity. This is illustrated in Fig. 10, which shows a line trace across the same CCD used in Fig. 9. Selected regions of the CCD were masked with 1-mm aluminum during irradiation so that several fluence regions could be achieved. The different mean dark-current values can be seen, but also the large number of dark-current spikes. Dark-current spikes were first reported for a proton irradiated CCD by Srour *et al.* [65]. They arise, in part, from single-particle inelastic nuclear reactions that deposit large amounts of displacement energy within a pixel but are rare enough that only small numbers of pixels are affected (at least at

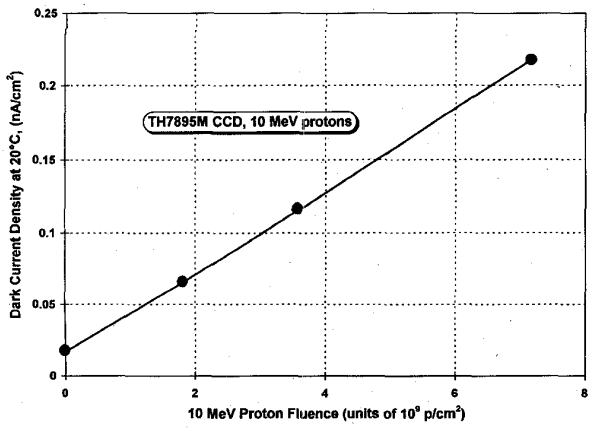

Fig. 9. Mean dark-current density versus fluence of 10-MeV protons for a TCS TH7895M MPP CCD.

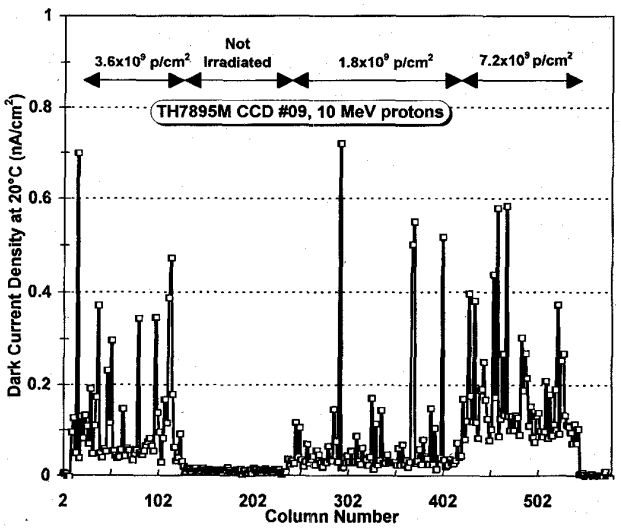

Fig. 10. Horizontal slice (row direction) across a dark image for the TH7895M device used in Figs. 9–11, showing the various fluence regions (achieved by masking during irradiation), and the presence of dark-current spikes.

low fluences). The nature of these inelastic reactions has been studied in detail by Burke [31], Dale *et al.* [32] and Chen *et al.* [66]. As an illustration, a 10-MeV proton will on average deposit 60 keV of damage energy in an inelastic reaction [32]. For a fluence of 5×10^9 p/cm^2 (fairly typical for a low Earth-orbit space mission), only 21% of pixels will contain an inelastic collision, as compared with ~500 elastic reactions/pixel for the same conditions, each of which would only deposit 0.18 keV.

Because of the small numbers of inelastic events, Poisson fluctuations are important, especially for small pixel geometries or for higher proton energies (where the mean damage energy increases to ~ 150 keV). Marshall *et al.* [67], [68], and Dale *et al.* [69] have studied the statistics of dark-current fluctuations in detail for CID's. They have developed an analytic description of the proton-induced damage distributions based on the interaction cross sections, the mean and variance of the damage energy deposited (for both elastic and inelastic events) and estimated values for the pixel-sensitive volume. The measured damage factor is used to determine the amount of dark current produced for each MeV of energy deposited. This analysis has also been successfully applied to EEV CCD's irradiated with 10-MeV protons [10]. The dark-current distributions, such as shown in Fig. 11, are found to be skewed, partly as a result of the infrequent, but highly damaging, inelastic nuclear reactions. For energies greater than roughly 50 MeV (or for small pixels), however, the ranges of the reaction recoil fragments approach the smallest dimension of the pixel, and the pixel-to-pixel damage variance increases rapidly. In this regime, a Monte Carlo approach is used to describe the damage energy distribution as discussed by Dale *et al.* [32].

B. Field Enhancement

There is another effect that occurs in any region of the depletion layer that contains a large electric field. This is known as field-enhanced emission and has been discussed by several authors [61], [67], [69]–[71]. This mechanism was identified in CCD's primarily based on the following observations: the activation energies for the high dark-current pixels were significantly reduced (Srour *et al.* [70] and Hopkinson *et al.* [71]) and the probability of a high dark-current pixel scales with NIEL (Marshall *et al.* [67] and Hopkins *et al.* [72]). For fields greater than about 10^4 V/cm, the emission from defects is increased because of tunneling effects.

For many devices, this field enhancement has a large impact on the dark-current distributions. For example, indications are that the histograms shown in Fig. 11 (for MPP CCD's) are more skewed than would be expected from the theory based on collision kinematics by Marshall *et al.* [68] and that this is due to field enhancement. Further evidence that field enhancement is occurring comes from an analysis based on extreme value statistics [72] (following [68]). This shows that the largest dark current spikes do not follow the same probability distribution as the smaller ones.

We thus have the situation that the dark current spikes can be produced either by a relatively frequent elastic event in an extremely small high-field region or a rare nuclear reaction anywhere within the entire sensitive volume. It is quite common for the largest spikes to have dark currents in the range 1–8 nA/cm^{-2} at 20°C (and for virtual phase CCD's, which tend to have particularly high fields, the amplitudes can be larger [70]). The number of large spikes, however, is usually of order 10 for a typical 288 × 384 pixel device for a fluence of $\sim 5 \times 10^9$ 10 MeV p/cm^2.

Dale *et al.* [40] have shown how analytic microdosimetry theory can be used in the case of field enhancement, but this requires knowing the field distribution within the device, and this is not usually available. The extreme value-statistics approach can give an idea of the extent of the problem, which in some cases can be ameliorated by simply reducing the gate voltage.

When dark-current generation is increased by field enhancement, it is also found that the temperature behavior is affected.

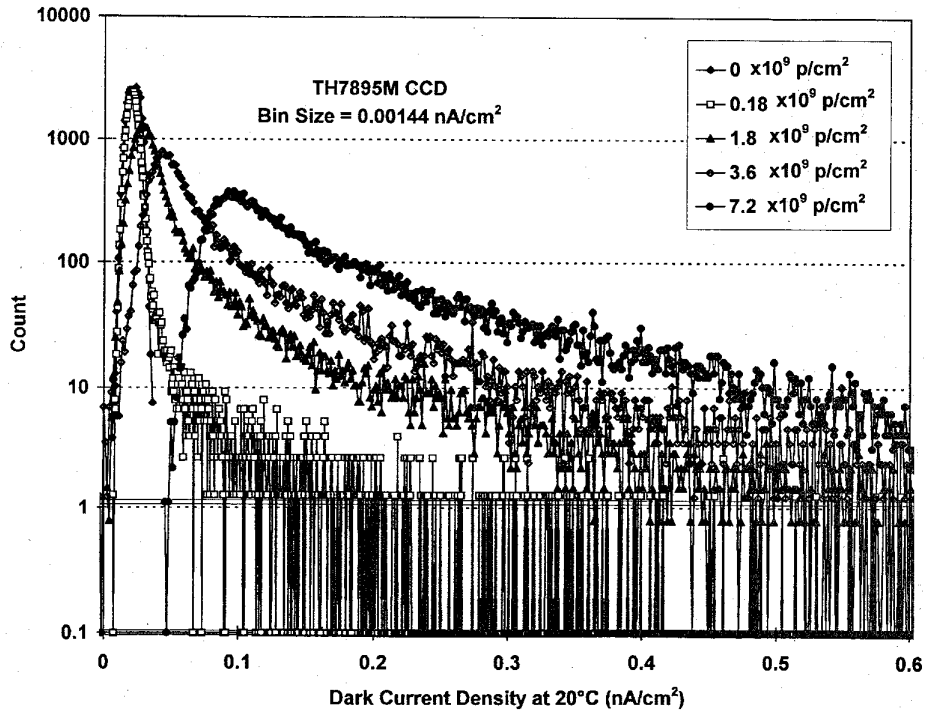

Fig. 11. Histograms of the dark-current density in each pixel for the four fluence regions of the CCD used in Fig. 9. The total count has been normalized to 1 $\times 10^5$ for each plot. Bin size = 0.00144 nA/cm^2.

Normally, the dark current follows the usual law for silicon and is proportional to T^{α} exp $(Eg/2\mathrm{kT})$ where Eg is the bandgap (itself temperature dependent) and α is an exponent (2 for bulk and 3 for surface dark current [73]). An approximation is to use a simple exponential function

$$\text{Dark current density} = \text{constant} \exp\left(\frac{E_{act}}{\mathrm{kT}}\right) \qquad (6)$$

where most of the pixels show an activation energy E_{act}) of ~0.64 eV. Equation (6) can, therefore, be used to extrapolate dark-current distributions to other temperatures. Field-enhanced spikes, however, show a slower change in amplitude with temperature, with some pixels showing an activation energy as low as 0.4 eV [70]. Work on the temperature behavior of dark-current spikes has shown that they are not caused by avalanche processes (the relevant volumes are too small for this mechanism).

C. Predicting Effects

To extrapolate ground-test data to mission environments, it is also necessary to understand the way in which the shape of dark-current distributions (such as those shown in Fig. 11) change with proton fluence (and energy). This has been discussed by Marshall *et al.* [68] for a CID. For the histograms of Fig. 11 (where it is believed that the tail is largely due to field-enhancement), a simple fit can be made assuming a Gaussian main peak whose half-width increases approximately as the square root of the fluence, and an exponential tail whose amplitude is proportional to fluence.

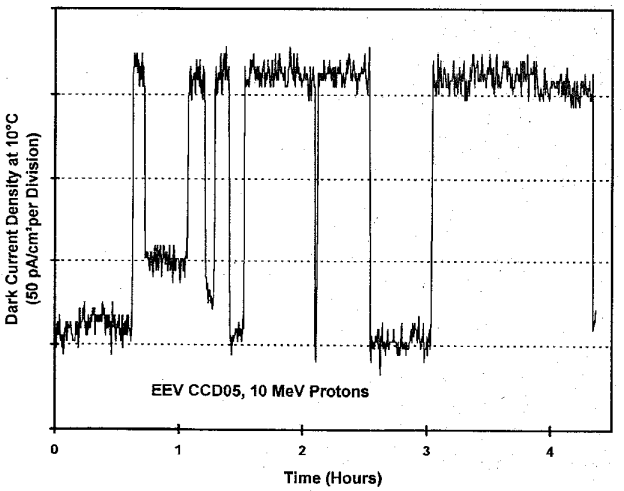

Fig. 12. After proton irradiation, some pixels show a time-varying dark current with the appearance of a random telegraph signal. This plot is for an EEV CCD02 device irradiated with 10-MeV protons, but similar results have been obtained with other devices and energies. These measurements were made at 10°C; at lower temperatures, the mean time constants for the high, and low states are increased.

The size of dark-current spikes is not normally affected by operating a device under surface inversion (which only changes the surface dark current), but the spike size does change with time after irradiation. Even if the device is stored at room temperature, it has been found that spike size often decreases over the first few weeks, but remains relatively stable thereafter (apart from switching effects, to

TABLE I
SUMMARY OF METHODS OF IMPROVING RADIATION TOLERANCE

Method	Effectiveness for protons in the Earth's natural environment
Instrument shielding	Effective for thicknesses up to (15 mm Al, but high energy protons cannot be stopped and secondary emission can be significant for thick shields of dense materials (e.g., T_a).
Choice of device architecture	CID's can be used if CTE problems are severe. Notched buried channels can be used to improve CTE for small signals. Large dark current spikes can be avoided if device internal electric fields are low. Optimization of active region thickness can improve response to transient events. Inverted mode (MPP) devices show negligible ionization-induced dark current-though at high doses the flatband shift can cause the substrate potential to become equipped and inversion to be lost. Flatband voltage shift can be reduced by appropriate choice of oxide technology.
CCD cooling	Effective in increasing the emission time of traps (can improve CTE) and in reducing dark current (in inverted mode, dark current performance will usually be limited by proton-induced dark current spikes).
Choice of clocking rate	Affects CTE and deferred charge, dark signal and transient hit rate (through the integration time).
Data Handling	Data- handling software can be used to discriminate against transient events and permanent dark current spikes. Measures can also be taken to correct for loss in CTE, though at the expense of noise performance.
Periodic heating (annealing)	Heating to temperatures in the range 100–150°C will anneal P–V centers and improve CTE and reduce dark current (provided other defects are not introduced).
'Fat zero'	Background charge or fat zero will improve CTE at the expense of increased shot noise. If the emission time is long (because of operation at low temperatures), then injection and flushing of charge has the same effect, without the noise penalty.
Defect Engineering	In principle it is possible to introduce controlled levels of impurities (such as oxygen) which can act as sinks for vacancies [76], e.g., the O–V complex (A center) has an energy level at 0.18 eV below the conduction band and is therefore not as close to mid-gap as the E-center). Another possibility is to use a dopant other than phosphorus for the buried channel. So far these techniques are in an exploratory stage and, to the authors' knowledge, good quality proton-hardened CCD's are not yet available.

be discussed below). These changes are interpreted as due to defect rearrangement or migration. For example, the E center is known to diffuse over time scales of weeks at room temperature [33] and might move into or out of high-field regions, thus changing the degree of field enhancement. The post irradiation behavior of CCD parameters has not been studied in detail but the results described earlier are believed to be representative of effects for the low dose-rate space environment. At high temperatures, the defects will anneal, and the spikes will disappear (e.g., the E center anneals at 150°C). Bias during irradiation is not known to affect the dark-current distributions.

D. Random Telegraph Signals

Recently, it has been discovered [10] that some pixels in proton-irradiated CCD's show a dark current that is not stable in time but switches between levels. This behavior gives the appearance of a random telegraph signal (RTS). Other authors [67], [69] had previously alluded to erratic dark currents, and subsequently the effect has been seen in several types of CCD [74], [75]. An example is shown in Fig. 12. Hopkins *et al.* [75] have shown that the probability of finding a pixel with RTS behavior is proportional to proton fluence, and it has recently been established that the occurrence probability increases with the elastic NIEL [72]. The RTS effect does not seem to depend on the state of surface inversion and may result from the reconfiguration of a defect within the bulk of the depletion layer, though the mechanism has not yet been identified. A mechanism such as electric field enhanced emission (or perhaps some cooperative effect between individual defects within a cluster) is required to explain the large amplitude of the dark-current fluctuations (which are usually in the range 0.01–0.1 nA/cm^2, at 20°C, though larger amplitudes have been reported for some devices [74]). The field-enhancement hypothesis also agrees with the finding [72] that a pixel is more likely to show RTS behavior if the mean dark level is already high (because of field-enhanced emission). The time constants for the switching behavior are on the order of several minutes at room temperature but rapidly increase as the CCD is cooled (an activation energy of 0.9 eV was found for the temperature range 10–25°C though a population of RTS pixels with switching times of several hours can still be found at −20°C [72]).

VI. DISCUSSION

A. Methods of Improving Radiation Tolerance

Several methods of mitigating the effects of radiation have been discussed earlier and these are summarized in Table I.

B. Future Work

A basic understanding of proton effects on silicon CCD's and similar devices is becoming established, thanks to an appreciable research effort over the past seven or eight years (in turn based on earlier work on neutron effects). There will always be a need, however, to gather test data relating to particular devices and applications and extrapolate these so as to predict effects for given missions. It should now be possible for engineers to use the research work referred to above so as to do this with some confidence, although there are still some areas where further work is needed (for example, to establish the mechanisms for random telegraph behavior). It has also become clear that, because of their sensitive nature,

CCD's are excellent devices for studying defects in silicon and also for verifying basic theories of microdosimetry. For example, Holland [46] has measured defect concentrations as low as 7×10^8 cm^{-3} by measuring CTI in CCD's, and Dale *et al.* [32] have discussed microdosimetry and the fluctuation effects that occur with small pixel sizes. Unfortunately, the increasing amount of ground-test data gathered over the past few years has not been matched by the level of data from in-flight measurements of CCD performance. Hence, there has been little opportunity to test whether our prediction methods are valid for the space environment. It is to be hoped that this situation will be improved with future CCD instruments. Finally, the study of radiation effects on imagers fabricated from materials other than silicon (for example HgCdTe) is a complex subject, still in its infancy, which is likely to increase its importance in the future.

ACKNOWLEDGMENT

Many of the examples discussed above have arisen from test campaigns funded by the European Space Agency and the study manager, B. Johlander, is thanked for his help and support. I. Hopkins (Sira/UCL Postgraduate Centre) is thanked for providing CTI data.

REFERENCES

[1] G. R. Hopkinson, "Radiation effects on solid state imaging devices," *Radiation Physics and Chemistry,* vol. 43, pp. 79–91, 1994.

[2] J. Pickel, "Novel devices and sensors," in *IEEE Nuclear and Space Radiation Effects Conf.,* Short Course Notes, Snowbird, UT, July 1993, pp. IV-I–IV-60.

[3] F. B. McLean, H. E. Boesch, and T. R. Oldham, "Charge generation, transport and trapping," in *Radiation Effects in MOS Devices and Circuits,* T. P. Ma and P. V. Dressendorfer, Eds. New York: Wiley-Interscience, 1989, ch. 3.

[4] J. Schwank, "basic mechanisms of radiation effects in the natural space environment," in *IEEE Nuclear and Space Radiation Effects Conference,* Tucson, AZ, July 1994, Short Course Notes, pp. II-1–II-109.

[5] J. R. Srour and J. M. McGarrity, "Radiation effects on microelectronics," *Proc. IEEE,* vol. 76, pp. 1443–1469, 1988.

[6] P. S. Winokur, "Radiation induced interface states," in *Radiation Effects in MOS Devices and Circuits,* T. P. Ma and P. V. Dressendorfer, Eds. New York: Wiley-Interscience, 1989, ch. 4.

[7] D. Braunig and F. Wulf, "Atomic displacement and total ionizing dose damage in semiconductors," *Radiation Physics and Chemistry,* vol. 43, pp. 105–127, 1994.

[8] J. Carbone, J. Zamowski, F. Arnold, and J. Hutton, "New low-noise random access, radiation resistant and large format charge injection device (CID) imagers," *Proc. SPIE,* vol. 1900, pp. 170–180, 1993.

[9] G. R. Hopkinson, "Radiation effects on CCD's for spaceborne acquisition and tracking applications," in *RADECS 91, IEEE Proc.,* 1992, pp. 368–372.

[10] ——, "Cobalt60 and proton radiation effects on large format, 2-D, CCD arrays for an earth imaging application," *IEEE Trans. Nucl. Sci.,* vol. 39, no. 6, pp. 2018–2025, 1992.

[11] N. S. Saks, "A technique for suppressing dark current generated by interface states in buried channel CCD imagers," *IEEE Electron Dev. Lett.,* vol. EDL-1, no. 7, pp. 131–133, 1980.

[12] J. Janesick, T. Elliott, R. Winzenread, J. Pinter, and R. Dyck, "Sandbox CCD's," *Proc. SPIE,* vol. 2415, pp. 2–42, 1995.

[13] B. Burke and S. A. Gajar, "Dynamic suppression of interface-state dark current in buried channel CCD's," *IEEE Trans. Electron Dev.,* vol. 38, no. 2, pp. 285–290, 1991.

[14] W. Van Toren and J. Bisschop, "Complete characterization of dark current in frame transfer image sensors," *Philips J. Res.,* vol. 48, pp. 207–231, 1994.

[15] J. F. Ziegler, J. P. Biersack, and U. Littmark, *The Stopping and Range of Ions in Solids.* Oxford: Pergamon Press, 1985, PC version developed by J. P. Biersack, and J. F. Ziegler, IBM-Research, Yorktown, NY.

[16] A. M. Kellerer, "Analysis of patterns of energy deposition—A survey of theoretical relations in microdosimetry theory," in *Proc. 2nd Symp. on Microdosimetry Theory,* H. G. Ebert, Ed., Brussels, Commission of the European Communities, 1969, pp. 107–135.

[17] E. A. Burke, J. J. Boyle, and H. J. Huemmler, "Gamma-induced noise in CCD's," *IEEE Trans. Nucl. Sci.,* vol. NS-28, pp. 4068–4073, 1981.

[18] V. E. Vickers, F. D. Shepherd, Jr., and E. A. Burke, "Ionizing radiation dosimetry and noise in small geometry devices," *IEEE Trans. Nucl. Sci.,* vol. NS-21, pp. 107–112, 1974.

[19] J. N. Bradford, "A distribution function for ion track lengths in rectangular volumes," *J. Appl. Phys.,* vol. 50, pp. 3799–3801, 1979.

[20] J. F. Ziegler and W. A. Landford, "The effect of sea level cosmic rays on electronic devices," *J. Appl. Phys.,* vol. 52, pp. 4305–4312, 1981.

[21] J. B. Langworthy, "Depletion region geometry analysis applied to single event sensitivity," *IEEE Trans. Nucl. Sci.,* vol. 36, no. 6, pp. 2427–2434, 1989.

[22] S. Kirkpatrick, "Modeling diffusion and collection of charge from ionizing radiation in silicon devices," *IEEE Trans. Electron Dev.,* vol. ED-26, pp. 1742–1753, 1979.

[23] G. R. Hopkinson, "Analytic modeling of charge diffusion in charge-coupled device imagers," *Opt. Eng.,* vol. 26, pp. 766–772, 1987.

[24] J. K. Pimbley and G. J. Michon, *IEEE Trans. Electron Dev.,* vol. ED-34, p. 294, 1987.

[25] M. A. Xapsos, E. A. Burke, P. Shapiro, and G. P. Summers, "Energy deposition and ionization fluctuations induced by ions in small sites-an analytical approach," *Radiation Research,* vol. 137, pp. 152–161, 1994.

[26] T. S. Lomheim, R. M. Shima, J. R. Angione, W. F. Woodward, D. J. Asman, R. A. Keller, and L. W. Schumann, "Imaging charge-coupled device (CCD) transient response to 17 and 50 MeV proton and heavy-ion irradiation," *IEEE Trans. Nucl. Sci.,* vol. 37, no. 6, pp. 1876–1885, 1990.

[27] K. J. McCarthy, A. Owens, A. Wells, W. Hajdas, F. Mattenberger, and A. Zehnder, "Measured and modeled CCD response to protons in the energy range 50–300 MeV," *Nucl. Inst. Meth.,* vol. A361, pp. 586–601, 1995.

[28] E. G. Stassinopoulos and J. P. Raymond, "The space radiation environment for electronics," *Proc. IEEE,* vol. 76, pp. 1423–1442, 1988.

[29] J. Letaw, "Space radiation code," Severn Communications Corp., 1989.

[30] G. P. Summers, "Displacement damage: Mechanisms and measurements," Short Course Notes, pp. IV-I–IV58, in *IEEE Nucl. Space Rad. Effects Conf.* New Orleans, LA, July, 1992.

[31] E. A. Burke, "Energy dependence of proton-induced displacement damage in silicon," *IEEE Trans. Nucl. Sci.,* vol. NS-33, no. 6, pp. 1276–1281, 1986.

[32] C. J. Dale, L. Chen, P. J. McNulty, P. W. Marshall, and E. A. Burke, "A comparison of Monte Carlo and analytical treatments of displacement damage in Si microvolumes," *IEEE Trans. Nucl. Sci.,* vol. 41, no. 6, pp. 1974–1983, 1994.

[33] G. D. Watkins and J. W. Corbett, "Defects in irradiated silicon: electron paramagnetic resonance and electron-nuclear double resonance of the Si–E center," *Phys. Rev.,* vol. 134, no. 5A, pp. 1359–1377, 1964.

[34] L. C. Kimmerling, M. T. Asom, J. L. Benton P. J. Drevinsky, and C. E. Caefer, "Interstitial defect reactions in silicon," *Materials Science Forum,* vol. 38–41, pp. 141–150, 1989.

[35] J. W. Corbett, J. C. Bourgoin, L. J. Cheng, J. C. Corelli, and Y. H. Lee, "The status of defect studies in silicon," *Inst. Phys. Conf. Series, no. 31,* pp. 1–11, 1977.

[36] J. Matheson, M. Robbins, and S. Watts, "Evidence that type inversion in N-type high-resistivity silicon diodes is due to a radiation-induced deep acceptor," *IEEE Trans. Nucl. Sci.,* vol. NS-42, no. 6, 1995.

[37] G. P. Summers, E. A. Burke, C. J. Dale, E. A. Wolicki, P. W. Marshall, and M. A. Gehlhausen, "Correlation of particle-induced displacement damage in silicon," *IEEE Trans. Nucl. Sci.,* vol. NS-34, no. 6, pp. 1134–1139, 1987.

[38] C. J. Dale and P. W. Marshall, "Displacement damage in Si imagers for space applications," *Proc. SPIE,* vol. 1447, pp. 70–86, 1991.

[39] M. Kurowkawa, T. Motobayashi, K. Ieki, S Shimoura, H. Murakawi, Y. Ikeda, S. Moriya, Y. Yanagisawa, and T. Nomura, "Radiation damage factor for ion-implanted silicon detectors irradiated with heavy ions," *IEEE Trans. Nucl. Sci.,* vol. 42, no. 3, pp. 163–166, 1995.

[40] C. J. Dale, P. W. Marshall, E. A. Burke, G. P. Summers, and G. E. Bender, "The generation lifetime damage factor, and its variance in silicon," *IEEE Trans. Nucl. Sci.,* vol. 36, no. 6, pp. 1872–1881, 1989.

[41] J. Janesick, G. Soli, T. Elliott, and S. Collins, "The effects of proton damage on charge-coupled devices.," *Charge-Coupled Dev., and Solid State Image Sensors II, Proc. SPIE,* vol. 1447, pp. 87–108, 1991.

[42] C. J. Dale, P. W. Marshall, B. Cummings, L. Shamey, and A. D. Holland, "Displacement damage effects in mixed particle environments for shielded spacecraft CCD's," *IEEE Trans. Nucl. Sci.,* vol. 40, no. 6, pp. 1628–1637, 1993.

[43] C. J. Dale, P. W. Marshall, G. P. Summers, and E. A. Wolicki, "Displacement damage equivalent to dose," *Appl. Phys. Lett.,* vol. 54, no. 5, pp. 451–453, 1989.

[44] J. D. E. Beynon and D. R. Lamb, *Charge-Coupled Devices and Their Applications.* New York: McGraw-Hill, 1980.

[45] S. G. Chamberlain, S. R. Karnasz, F. Ma, W. D. Washkurak, M. Farrier, and P. T. Jenkins, "A 26.2 Million pixel CCD image sensor," *Proc. SPIE,* vol. 1900, pp. 181–192, 1993.

[46] A. Holland, "The effect of bulk traps in proton-irradiated EEV CCDs," *Nucl. Inst. Meth.,* vol. A326, pp. 335–343, 1993.

[47] R. D. McGrath, J. Doty, G. Lupino, G. Ricker, and J. Vallerga, "Counting of deep-level traps using a charge-coupled device," *IEEE Trans. Electron Dev.,* vol. ED-34, pp. 2555–2557, 1987.

[48] R. G. Murowinski, G. Linzhuang, and M. J. Deen, "Effects of space radiation damage, and temperature on the noise in CCD's, and LDD MOS transistors," *IEEE Trans. Nucl. Sci.,* vol. 40, no. 3, pp. 288–294, 1993.

[49] ———, "Effects of space radiation damage, and temperature on CCD noise for the Lyman fuse mission," *Proc. SPIE,* vol. 1953, pp. 71–81, 1993.

[50] M. Robbins, "Radiation damage effects in charge coupled devices," Ph.D. dissertation, Brunel University, 1992.

[51] M. V. Wadsworth, S. R. Borello, J. Dodge, R. Gooch, W. McCardel, G. Nado, and M. D. Shilhanek, "Monolithic CCD imagers in HgCdTe," *IEEE Trans. Electron Dev.,* vol. 42, no. 2, pp. 244–250, 1995.

[52] G. R. Hopkinson, C. J. Baddiley, D. R. P. Guy, and J. E. Parsons, "Total dose, and proton testing of a commercial HgCdTe array," *IEEE Trans. Nucl. Sci.,* vol. 41, no. 6, pp. 1966–1973, 1994.

[53] J. Cluzel, A Guiga, R. Tronel, and M. Vilain, "Radiation effects on CCD" in *RADECS 91, IEEE Proc.,* 1992, pp. 327–332.

[54] J. R. Waterman and R. A. Schiebel, "Ionizing radiation effects in N-channel HgCdTe MISFET's with anodic sulphide passivation," *IEEE Trans. Nucl. Sci.,* vol. NS-34, no. 6, pp. 1597–1601, Dec. 1987.

[55] A. D. Holland, A. Holmes-Seidle, B. Johlander, and L. Adams, "Techniques for minimizing space proton damage in scientific charge coupled devices," *IEEE Trans. Nucl. Sci.,* vol. 38, no. 6, pp. 1663–1670, 1991.

[56] K. C. Gendreau, G. Y. Prigozhin, R. K. Huang, and M. W Bautz, "A technique to measure trap characteristics in CCD's using X-rays," *IEEE Trans. Electron Dev.,* vol. 42, no. 11, pp. 1912–1917, 1995.

[57] M. S. Robbins, T. Roy, and S. J. Watts, "Degradation of the charge transfer efficiency of a buried channel charge coupled device due to radiation damage by a beta source," in *RADECS 91, IEEE Proc.,* 1992, pp. 327–332, 1992.

[58] I. Zayor, I. Chapman, D. Duncan, G. Kelly, and K. Mitchell, "Results from proton damage tests on the Michelson Doppler imager CCD for SOHO," *Proc. SPIE,* vol. 1900, pp. 97–103, 1993.

[59] I. H Hopkins, G. R. Hopkinson, and B. Johlander, "Proton-induced charge transfer degradation in CCD's for near-room temperature applications," *IEEE Trans. Nucl. Sci.,* vol. 41, no. 6, pp. 1984–1990, 1994.

[60] A. Mohsen and M. F. Tompsett, "The effects of bulk traps on the performance of bulk channel charge-coupled devices," *IEEE Trans. Electro Dev.,* vol. ED-21, no. 11, pp. 701–712, 1974.

[61] E. K. Banghart, J. P. Lavine, E. A. Trabka, E. T. Nelson, and B. C. Burkey, "A model for charge transfer in buried channel charge-coupled devices at low temperature, *IEEE Trans. Electron Dev.,* vol. 38, no. 3, pp. 1162–1174, 1991.

[62] D. J. Burt, "Development of X-ray CCD's," in *Proc. ESA Symp. on Photon Detectors for Space Instrumentation,* Nov. 1992, ESA SP-356, pp. 57–67.

[63] A. D. Holland, "Annealing of proton-induced displacement damage in CCD's for space use," in *Inst. Phys. Conf. Ser.,* 1991, vol. 121, pp. 33–40.

[64] J. Janesick, T. Elliott, R. Bredthauer, C. Chandler, and B. Burke, "Fano-noise limited CCD's," *X-ray Instrumentation in Astronomy II, Proc. SPIE,* vol. 982, pp. 70–95, 1988.

[65] J. R. Srour, R. A. Hartmann, and K. S. Kitazaki, "Permanent damage produced by single proton interactions in silicon devices," *IEEE Trans. Nucl. Sci.,* vol. NS-33, no. 6, pp. 1597–1604, 1986.

[66] L. Chen, P. J. McNulty, W. G. Abdel-Kader, T. L. Miller, and D. A. Thompson, "Single, and multiple proton-induced NIEL events in silicon," *RADECS 93, IEEE Proc.,* pp. 526–531, 1994.

[67] P. W. Marshall, C. J. Dale, E. A. Burke, G. P. Summers, and G. E. Bender, "Displacement damage extremes in silicon depletion regions," *IEEE Trans. Nucl. Sci.,* vol. 36, no. 6, pp. 1831–1839, 1989.

[68] P. W. Marshall, C. J. Dale, and E. A. Burke, "Proton-induced displacement damage distributions in silicon microvolumes," *IEEE Trans. Nucl. Sci.,* vol. 37, no. 6, pp. 1776–1783, 1990.

[69] C. J. Dale, P. W. Marshall, and E. A. Burke, "Particle-induced dark current fluctuations in focal plane arrays" *IEEE Trans. Nucl. Sci.,* vol. 37, no. 6, pp. 1784–1791, 1990.

[70] J. R. Srour, and R. A. Hartmann, "Enhanced displacement damage effectiveness in irradiated silicon devices," *IEEE Trans. Nucl. Sci.,* vol. NS-36, no. 6, pp. 1825–1830, 1989.

[71] G. R. Hopkinson, and Ch. Chlebek, "Proton damage effects in an EEV CCD imager," *IEEE Trans. Nucl. Sci.,* vol. 36, no. 6, pp. 1865–1871, 1989.

[72] I. H. Hopkins and G. R. Hopkinson, "Further measurements of random telegraph signals in proton-irradiated CCD's," *IEEE Trans. Nucl. Sci.,* vol. 42, no. 6, pp. 2074–2081, 1995.

[73] G. R. Hopkinson, "Radiation-induced dark current increases in CCDs," *RADECS 93, IEEE Proc.,* pp. 401–408, 1994.

[74] T. L. Miller, D. A. Thompson, M. B. Elzinga, T.-H. Lee, B. C. Passenheim, and R. E. Leadon, "Experimental evaluation of high speed CCD imager radiation effects using Co60, and proton radiation," in *1993 IEEE Radiation Effects Data Workshop,* IEEE, 1994, pp. 56–63.

[75] I. H. Hopkins and G. R. Hopkinson, "Random telegraph signals from proton-irradiated CCD's," *IEEE Trans. Nucl. Sci.,* vol. 40, no. 6, pp. 1567–1574, 1993.

[76] M.-A. Trauwaert, J. Vanhellemont, E. Simoen, C. Claeys, B. Johlander, and L. Adams, "Study of electrically active lattice defects in Cf-252, and proton irradiated silicon diodes," *IEEE Trans. Nucl. Sci.,* vol. 39, no. 6, pp. 1747–1753, 1992.